

*Letter to the Editor***Evidence for an expanding molecular superbubble in M 82**

Axel Weiß, Fabian Walter, Nikolaus Neininger, and Uli Klein

Radioastronomisches Institut der Universität Bonn, Auf dem Hügel 71, D-53121 Bonn, Germany

Received 23 February 1999 / Accepted 6 April 1999

Abstract. We present evidence for an expanding superbubble in M 82 (diameter: ≈ 130 pc, expansion velocity: ≈ 45 km s $^{-1}$, mass: $\approx 8 \cdot 10^6 M_{\odot}$). It is seen in the $^{12}\text{CO}(J = 1 \rightarrow 0)$, $^{12}\text{CO}(J = 2 \rightarrow 1)$, $^{13}\text{CO}(J = 1 \rightarrow 0)$ and $\text{C}^{18}\text{O}(J = 1 \rightarrow 0)$ lines. The superbubble is centred around the most powerful supernova remnant, 41.9+58. The CO observations show that the molecular superbubble already broke out of the disk. This scenario is supported by ROSAT HRI observations which suggest that hot coronal gas originating from inside the shell is the main contributor to the diffuse X-ray outflow in M 82. We briefly discuss observations of the same region at other wavelengths (radio continuum, optical, H I, X-rays, ionized gas). From our spectral line observations, we derive a kinematic age of about 10^6 years for the superbubble. Using simple theoretical models, the total energy needed for the creation of this superbubble is of order 2×10^{54} ergs. The required energy input rate (0.001 SN yr $^{-1}$) is reasonable given the high supernova (SN) rate of ≈ 0.1 SN yr $^{-1}$ in the central part of M 82. As much as 10% of the energy needed to create the superbubble is still present in form of the kinetic energy of the expanding molecular shell. Of order 10% is conserved in the hot X-ray emitting gas emerging from the superbubble into the halo of M 82. This newly detected expanding molecular superbubble is believed to be powered by the same objects that also lie at the origin of the prominent X-ray outflow in M 82. It can therefore be used as an alternative tool to investigate the physical properties of these sources.

Key words: ISM: bubbles – galaxies: individual: M 82 – galaxies: ISM – galaxies: kinematics and dynamics – galaxies: starburst – X-rays: ISM

1. Introduction

M 82 is the best studied nearby starburst galaxy ($D = 3.25$ Mpc). The central few hundred parsecs of this galaxy are heavily obscured by dust and gas which hides the central starburst region against direct observations at optical wavelengths. Evidence for strong star-forming activity in the central region comes from radio (e.g. Kronberg et al. 1981) and infrared observations (e.g. Telesco et al. 1991) and also from the prominent

bipolar outflow visible in H α (e.g. Bland & Tully 1988, McKeith et al. 1995, Shopbell & Bland–Hawthorn 1998) and in X-rays (e.g. Bregman et al. 1995). The massive star formation (SF) is believed to be fuelled by the large amount of molecular gas which is present in the centre of M 82.

On the other hand, SF effects the distribution and kinematics of the surrounding interstellar medium (ISM). Recent millimetre continuum observations (Carlstrom & Kronberg 1990) suggested that the HII regions in M 82 have swept up most of the surrounding neutral gas and dust into dense shells. This is in agreement with the standard picture: shells are created by young star-forming regions through strong stellar winds of the most massive stars in a cluster and through subsequent type-II supernovae (e.g. Tenorio-Tagle & Bodenheimer 1991). These processes are thought to blow huge cavities filled with coronal gas into their ambient ISM (e.g. Cox & Smith 1974, Weaver et al. 1977). This hot interior is then believed to drive the expansion of the outer shell of swept-up material.

Once superbubbles reach sizes that are comparable to the thickness of a galaxy's disk, the bubble will eventually break out into the halo. This then leads to an outflow of the hot gas with velocities much higher than the expansion of the shell within the disk of the galaxy. In the following we present evidence for a molecular superbubble in M 82 which already broke out of the disk and seems to contribute significantly to the well-known prominent outflow of M 82.

2. Observations*2.1. Molecular lines*

For our analysis we used the $^{12}\text{CO}(J = 1 \rightarrow 0)$ data cube obtained by Shen & Lo (1995) with the BIMA array (spatial resolution: $2.5''$) and the $^{13}\text{CO}(J = 1 \rightarrow 0)$ data cube from Neininger et al. (1998) observed with the Plateau de Bure interferometer (PdBI) (spatial resolution: $4.2''$). In addition, we used unpublished PdBI data of the $^{12}\text{CO}(J = 2 \rightarrow 1)$ and $\text{C}^{18}\text{O}(J = 1 \rightarrow 0)$ transitions. These observations were carried out in April 1997 in the CD configuration, resulting in a spatial resolution of $1.4'' \times 1.2''$ ($^{12}\text{CO}(J = 2 \rightarrow 1)$) and $3.7'' \times 3.5''$ ($\text{C}^{18}\text{O}(J = 1 \rightarrow 0)$), and a velocity resolution of 3.3 km s $^{-1}$ and 6.8 km s $^{-1}$, respectively. In order to increase the sensitivity to extended CO emission we combined

Send offprint requests to: A.Weiß(aweiss@astro.uni-bonn.de)

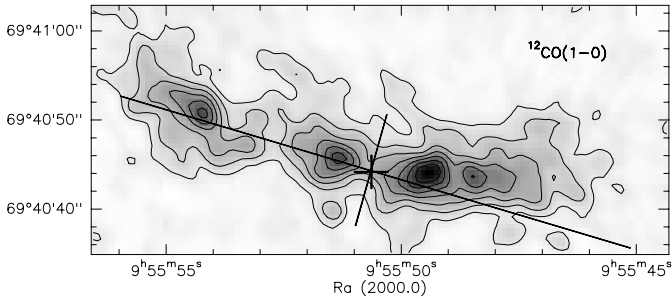


Fig. 1. Integrated ^{12}CO line emission from Shen & Lo (1995). The lines along the major and minor axis of M 82 indicate the orientations of the pv-diagrams shown in Figs. 2 and 3. The cross marks the position of SNR 41.9+58.

the $^{12}\text{CO}(J = 2 \rightarrow 1)$ data cube with single dish measurements obtained with the IRAM 30m telescope. These observations were carried out in May 1998. The combination is essential for this particular study because the receding part of the superbubble is only marginally visible in the mere interferometer maps. A full account of the data reduction will be given elsewhere.

2.2. Evidence for an expanding superbubble

Fig. 1 shows the integrated ^{12}CO line emission published by Shen & Lo (1995). The cross corresponds to the position of the supernova remnant 41.9+58 (SNR 41.9+58) which is the strongest cm continuum point-source in M 82 (Kronberg et al. 1981). It is considered to be the aftermath of a ‘hypernova’, which exhibits a radio luminosity 50–100 times greater than typical for type-II SNe (Wilkinson & de Bruyn 1990). The line along the major axis indicates the orientation of the position-velocity (pv) diagrams shown in Fig. 2.

The pv-cut is orientated in such a way that the signature of the expanding superbubble is visible most distinctly. The angular axis of the pv diagrams correspond to the offset in arcseconds from SNR 41.9+58. Besides a constant velocity gradient (cf. Shen & Lo 1995) the pv-diagrams show an expanding ring-like feature centred on SNR 41.9+58, with a central velocity of $V_{\text{lsr}} \approx 150 \text{ km s}^{-1}$. The approaching velocity component of the ring is clearly seen in all cubes and is centred at 100 km s^{-1} . The receding component is only marginally visible in the $^{13}\text{CO}(J = 1 \rightarrow 0)$ and $\text{C}^{18}\text{O}(J = 1 \rightarrow 0)$ lines; its central velocity is about 190 km s^{-1} . An enlargement of the pv-diagram along the major axis is shown in Fig. 3 (left). From this diagram we estimate the radius of the ring to be $(65 \pm 5) \text{ pc}$ and the expansion velocity $(45 \pm 5) \text{ km s}^{-1}$. A pv-diagram along the minor axis centred on SNR 41.9+58 is presented in Fig. 3 (right). The orientation of the cut is shown in Fig. 1.

Fig. 3 (right) reveals two emission features centred at the position of SNR 41.9+58, which correspond to the approaching ($v \approx 100 \text{ km s}^{-1}$) and the receding component ($v \approx 190 \text{ km s}^{-1}$) of the expanding superbubble. Hardly any CO emission with a velocity between $v = 100 \text{ km s}^{-1}$ and $v = 190 \text{ km s}^{-1}$ is found south and north of SNR 41.9+58. The pv-diagrams therefore show that the expanding molecular shell has

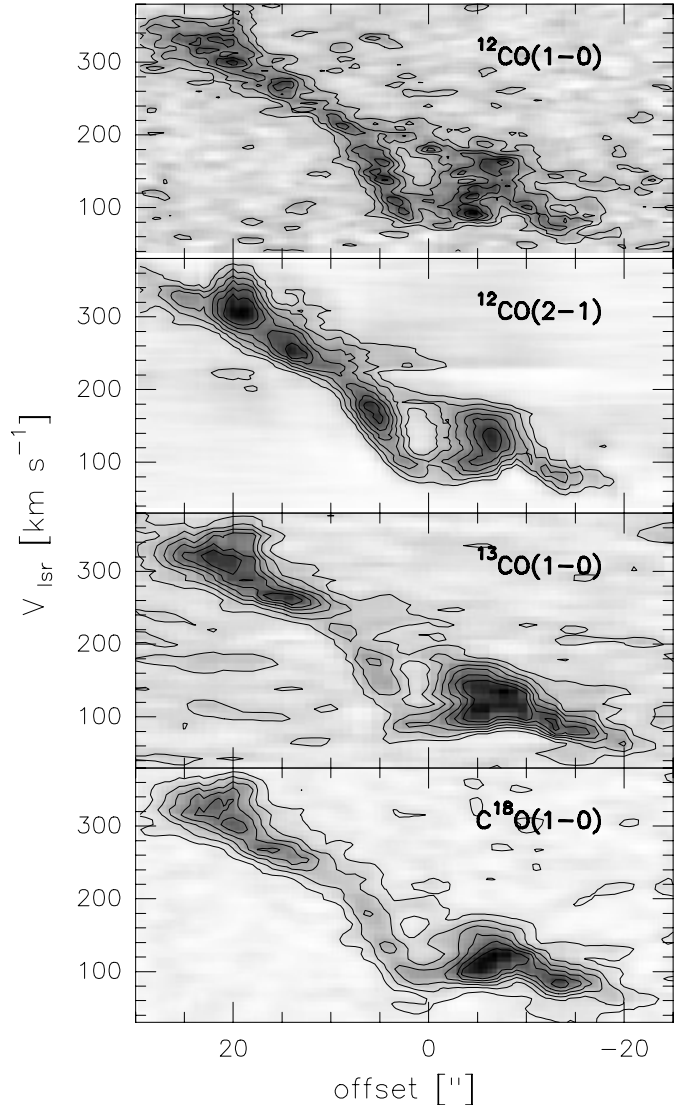


Fig. 2. The pv-diagrams along the major axis of M 82 (orientation shown in Fig. 1) for the $^{12}\text{CO}(J = 1 \rightarrow 0)$, $^{12}\text{CO}(J = 2 \rightarrow 1)$, $^{13}\text{CO}(J = 1 \rightarrow 0)$ and $\text{C}^{18}\text{O}(J = 1 \rightarrow 0)$ cubes. The slice is centred on SNR 41.9+58.

already broken out of the disk and now only shows the signature of an expanding molecular ring. It should be noted that the remaining molecular gas in M 82 shows clear solid-body rotation.

2.3. Other wavelengths

Radio continuum observations: Radio continuum observations at 408 MHz by Wills et al. (1997) unveiled a prominent ‘hole’ of approximately 100 pc diameter around SNR 41.9+58 which they attribute to free-free absorption. They propose that this feature is due to absorption by a large H II region that has been photoionized by a cluster of early-type stars of which the progenitor of SNR 41.9+58 was originally a member. It should be noted, however, that SNR 41.9+58 is only about 50 years old

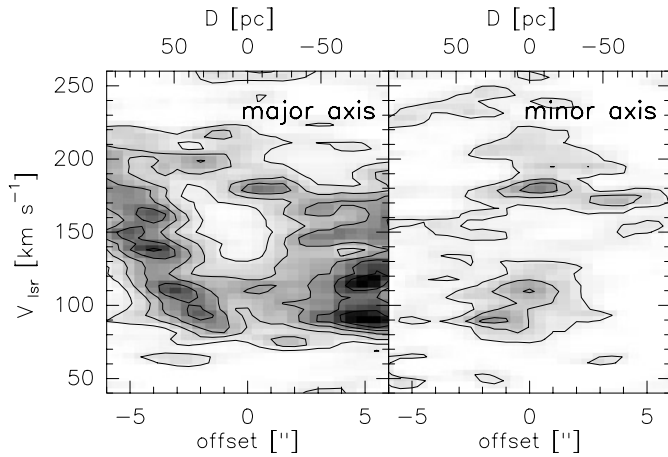


Fig. 3. The p - v -diagrams for the $^{12}\text{CO}(J = 1 \rightarrow 0)$ transition along the major and minor axis of M 82. The spatial axis for each diagram is centred on SNR 41.9+58. The p - v -diagram along the major axis is an enlargement of Fig. 2 (top). The orientation of the cut along the minor axis is indicated in Fig. 1.

(Wilkinson & de Bruyn 1990) and therefore cannot be the source that drives the expansion of the superbubble. But its presence supports the scenario that the expanding molecular superbubble is powered by an interior stellar cluster.

Neutral hydrogen (HI): HI emission line studies show that the central kpc of M 82 is dominated by absorption (Yun et al. 1993), which makes it difficult to study the HI kinematics in the central part of the galaxy. Recent HI absorption studies against supernova remnants in M 82 by Wills et al. (1998) disclosed two absorption features against SNR 41.9+58. The velocities of the components are $87 \pm 7 \text{ km s}^{-1}$ and $200 \pm 7 \text{ km s}^{-1}$. The HI component at 87 km s^{-1} can be attributed to the approaching component of the expanding superbubble. The absorption feature at 200 km s^{-1} , if associated with the receding part, seems to contradict the hypothesis that SNR 41.9+58 is located within the expanding superbubble. However, the velocity resolution of the absorption study was rather poor (26.4 km s^{-1}) and other explanations cannot be ruled out at this point.

Optical observations: Optical observations of the centre of M 82 suffer heavily from light absorption by the prominent dust lanes, rendering an optical analysis of this particular region impossible. HST V- and I-band images of the centre of M 82 (O’Connell et al. 1995) do not reveal any optical sources in the vicinity of SNR 41.9+58. The prominent $\text{H}\alpha$ outflow is visible north and south of the absorbing dust lane (Bland & Tully 1988, McKeith et al. 1995, Shopbell & Bland-Hawthorn 1998). The orientation of its filaments suggests that the $\text{H}\alpha$ outflow emerges at least partly from the location of the molecular superbubble.

X-ray observations: Fig. 4 shows an overlay of archival ROSAT HRI X-ray data (Bregman et al. 1995) onto the CO emission. To emphasize the diffuse, extended X-ray outflow

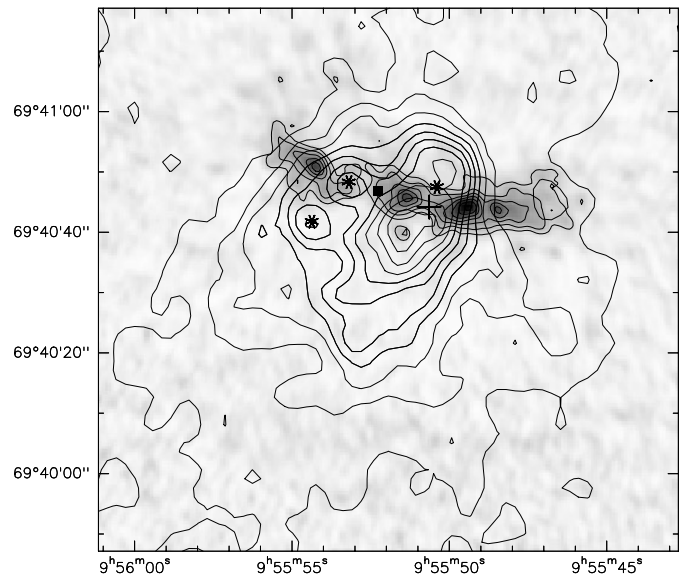


Fig. 4. Integrated $^{12}\text{CO}(J = 1 \rightarrow 0)$ line emission of M 82 (greyscale). The contour map represents the diffuse X-ray emission without the strongest point-source in the core of M 82 as observed by the ROSAT HRI. The three X-ray point-sources are marked with a star, the position of SNR 41.9+58 by a cross; the centre of M 82 ($2.2 \mu\text{m}$ peak) is indicated by a filled box.

we subtracted a model of the brightest X-ray point source at $\alpha = 9^{\text{h}}55^{\text{m}}50^{\text{s}}.4$, $\delta = 69^{\circ}40'47.5''$ (J2000.0) and smoothed the residual image to a $6''$ resolution. The positions of the three point sources in the field are marked with stars, SNR 41.9+58 is marked by a cross (see also Bregman et al.). The overlay shows that most of the diffuse X-ray emission arises from the vicinity of SNR 41.9+58. The shape of the diffuse emission is elongated, extending several arcminutes along the minor axis of the galaxy. Model calculations by Bregman et al. show that the emission is consistent with an outflow of heated material from the central region coincident with the position of the expanding molecular superbubble.

We estimate an upper limit for the energy still present in the hot gas emerging from the superbubble. For the calculation we adopt a density $n = 0.2 \text{ cm}^{-3}$ and a temperature $kT = 1 \text{ keV}$ for the central region (Bregman et al.) as an upper limit for the mean values in the outflow. We find an upper limit for the energy of $E_{\text{gas}} \leq 2.7 \times 10^{53} \text{ ergs}$ present in a cylindrical volume with $r = 130 \text{ pc}$ and $z = 550 \text{ pc}$ centred on the superbubble. From the thickness of the molecular disk of M 82 ($\approx 90 \text{ pc}$) and the expansion velocity of the superbubble we estimate a time elapsed since outbreak of $\tau \approx 3 \times 10^5 \text{ yr}$. The required outflow velocity to reach the observed height above the disk therefore is $v \approx 1000 \text{ km s}^{-1}$. This value is comparable with estimates based on particle aging as derived from radio continuum observations (Sequist et al. 1985) and measured outflow velocities in $\text{H}\alpha$ (McKeith et al. 1995).

Ionized gas: Most studies of the ionized gas in M 82 unfortunately do not provide sufficient spatial and spectral resolution to

reveal details of the region under study. A high-resolution study of the Ne II emission line has been published by Achtermann & Lacy (1995). The integrated line emission in the south-western region of M 82 shows a similar double-peaked feature centred on SNR 41.9+58 as traced by the CO. The p_v -cut along the major axis clearly shows a disturbed velocity field in the vicinity of SNR 41.9+58. The approaching side of the expanding superbubble at 95 km s^{-1} is clearly visible while the receding side at 190 km s^{-1} is only marginally seen. The diameter of the Ne II shell ($\approx 100 \text{ pc}$) seems to be somewhat smaller than the corresponding CO feature, suggesting that the inner part of the expanding superbubble is ionized. Similar features are visible in the distribution and the kinematics of the H41 α emission line (Seaquist et al. 1996). The Ne II distribution might represent the transition from the hot coronal gas with a temperature of several 10^6 K towards the cold molecular rim of the superbubble.

3. Discussion

The picture that emerges from the observations presented above is the following: a major SF event at the centre of what today shows up as the prominent expanding molecular superbubble created a cavity filled with coronal gas by the combined effects of strong stellar winds and SN explosions. The pressure of the hot-gas interior drove the expansion of the shell of swept-up material until it broke out of the disk. The subsequent outflow of hot material today shows up as diffuse X-ray emission and contributes to the prominent H α filaments.

From the observational parameters of the expanding superbubble (expansion velocity and diameter) we estimate a kinematic age of the superbubble of 1×10^6 years. The kinematic age is an upper limit for the actual age since the superbubble is most probably decelerating. We use Chevalier's equation (Chevalier 1974) to derive the amount of energy needed to create the expanding superbubble. Since Chevalier's equation applies to H I shells only we corrected the energy input by a factor of 2 to correct for the difference in mass between H $_2$ and H. We estimate an ambient H $_2$ density prior to the creation of the shell of order 120 cm^{-3} . This is done by converting the $^{12}\text{CO}(J = 1 \rightarrow 0)$ line integral to H $_2$ column density using a conversion ratio of $N(\text{H}_2)/W(\text{CO}) = 1.2 \times 10^{20} \text{ cm}^{-2} \text{ K}^{-1} \text{ km}^{-1} \text{ s}$ (Smith et al. 1991) and estimating the volume of the region from which material was swept up to be cylindrical with $z = 100 \text{ pc}$ and $r = 65 \text{ pc}$. We derive a total energy of order 2×10^{54} ergs, which corresponds to an energy equivalent of approximately 1000 type-II SNe and the strong stellar winds of their progenitors. With the estimate for the age of the superbubble this leads to a SN rate of 0.001 SN yr^{-1} for the central stellar cluster. This is a reasonable number given the fact that the SN rate in the central part of M 82 was estimated to be about 0.1 SN yr^{-1} (Kronberg et al. 1981). The total H $_2$ mass of the superbubble is about $8 \times 10^6 M_{\odot}$. Less than 15% of the total

energy is still present in the hot gas which emerges from the superbubble; the fraction of kinetic energy of the molecular superbubble is about 10% ($E_{\text{kin}} \approx 1.6 \times 10^{53}$ ergs). It should be noted, however, that the numbers given above are only order of magnitude estimates.

The wealth of observations presented above indicates that the region under study represents an unusually active segment of the starburst in M 82. The finding of an expanding molecular superbubble in this particular region supports this view and provides clear evidence for a footprint of violent SF in the ISM of M 82. Furthermore the analysis of the molecular superbubble presents an alternative tool to investigate the energy release of the central source which drives the X-ray and contributes to the H α outflow.

Acknowledgements. A.W. and F.W. acknowledge DFG grant III GK-GRK 118/2. We thank J. Shen and K.Y. Lo for making available their CO data, J. Kerp for his help on the ROSAT data and the referee, P. Kronberg, for helpful comments. We acknowledge the IRAM staff for carrying out the observations and the help provided during the data reduction.

References

- Achtermann J.M., Lacy J.H., 1995, ApJ 439, 163
 Bland J., Tully B., 1988, Nature 334, 43B
 Bregman J.N., Schulman E., Tomisaka K., 1995, ApJ 439, 155
 Carlstrom, J.E., Kronberg, P.P., 1990, ApJ 366, 422
 Chevalier R.A., 1974, ApJ 188, 501
 Cox D.P., Smith B.W., 1974, ApJ 189, L105
 Dietz K., Smith J., Hackwell J.A., Gehrz D.R., Grasdalen G.L., 1986, AJ 91, 758
 Kronberg, P.P., Biermann P., Schwab F.R., 1981, ApJ 291, 693
 McKeith, C.D., Greve, A., Downes D., Prada, F., 1995, A&A 293, 703
 Neininger N., Guélin M., Klein U., Wielebinski R., 1998, A&A 339, 737
 O'Connell R.W., Gallagher III J.S., Hunter D.A. Colley W.N., 1995, ApJ 446, L1
 Seaquist E.R., Bell M.B., Bignell, R.C., 1985, ApJ 294, 546
 Seaquist E.R., Carlstrom J.E., Bryant P.M., Bell M.B., 1996, ApJ 465, 691
 Shen J., Lo K.Y., 1995, ApJ 445, L99
 Shopbell P.L., Bland-Hawthorn J., 1998, ApJ 493, 129
 Smith P.A., Brand P.W.J.L., Mountain C.M., Puxley P.J., Nakai N., 1991, MNRAS 252, 6
 Tesesco C.M., Campins H., Joy M., Dietz K., Decher R., 1991, ApJ 369, 135
 Tenorio-Tagle G., Bodenheimer P., 1988, ARA&A, 26, 145
 Weaver R., McCray O., Castor J., Shapiro P., Moore R., 1977, ApJ 218, 377
 Wilkinson P.N., de Bruyn A.G., 1990, MNRAS 242, 529
 Wills K.A., Pedlar A., Muxlow T., Wilkinson P.N., 1997, MNRAS, 291, 517
 Wills K.A., Pedlar A., Muxlow T., 1998, MNRAS 298, 347
 Yun M.S., Ho P.T.P., Lo K.Y., 1993, ApJ 411, L17